NASA Contractor Report 3481

Design of Prototype Charged Particle Fog Dispersal Unit

Frank G. Collins, Walter Frost,
and Philip Kessel
FWG Associates, Inc.
Tullahoma, Tennessee

Prepared for
George C. Marshall Space Flight Center
under Contract NAS8-33541

National Aeronautics
and Space Administration

**Scientific and Technical
Information Branch**

1981

ACKNOWLEDGMENTS

The work reported herein was supported by the National Aeronautics and Space Administration, Marshall Space Flight Center, Space Sciences Laboratory, Atmospheric Sciences Division, under Contract NAS8-33541.

The authors are indebted to Mr. A. Richard Tobiason of the Office of Aeronautics and Space Technology (OAST), NASA Headquarters, Washington, D. C., for his support of this research. Special thanks are given to Mr. Dennis W. Camp of Marshall Space Flight Center who was the scientific monitor of the program and provided considerable technical advice and input to the final documentation. Also, the authors are appreciative of the technical discussions with various personnel of the FAA, Naval Research Laboratories, and Energy Innovations, Inc.

TABLE OF CONTENTS

SECTION		PAGE
1.0	INTRODUCTION	1
2.0	DESIGN OF PROTOTYPE CHARGED PARTICLE FOG DISPERSAL UNIT	2
	2.1 Previous Designs	2
	2.2 Description of Prototype Unit	2
	2.3 Design of Prototype Unit	10
3.0	DRAWINGS OF PROTOTYPE CHARGED PARTICLE FOG DISPERSAL UNIT	20
4.0	DESIGN OF VERIFICATION EXPERIMENTS FOR FOG DISPERSAL UNIT	24
5.0	CONCLUDING REMARKS	27
REFERENCES		28
APPENDIX--BIBLIOGRAPHY OF WORK RELATED TO ELECTROFLUID DYNAMIC POWER GENERATION		31

LIST OF ILLUSTRATIONS

FIGURE	TITLE	PAGE
1	Prototype Fog Dispersal Nozzle	5
2	Schematic of Charge Spray Nozzle	8
3	Nozzle Controls	9
4	Typical Electrode Configuration of EFD Test Rig [25]	11
5	Current as a Function of the Needle Position in Nozzle [25]	12
6	Corona Needles	13
7	Configuration Factor of G for Both the Two-Dimensional and Axisymmetric Geometries [26]	15
8	Lines of Constant Normalized Power as a Function of M* and V for a Gas with k = 1.4. The field strength at the generator entrance is E_b [26]	16
9	Cross Section of Prototype Nozzle	21
10	Details of Prototype Nozzle	22
11	Details of Prototype Fog Dispersal System	23

LIST OF TABLES

TABLE	TITLE	PAGE
1	Features of Prototype Nozzle	3
2	Nozzle Characteristics	6
3	Characteristics of Nozzle Droplets	13
4	Corona Scaling Laws	18
5	Quantities to be Measured	25

NOMENCLATURE

D	Normalized charge density
E_b	Field strength at the generator entrance
E_{bo}	Gas breakdown electric field
G	Configuration factor
h	Channel length
I	Current at attractor
I_j	Jet current
M	Mach number of gas
M^*	Mach number based on local speed of sound
P	Pressure
R	Channel radius
V	Gas velocity
$\overline{V}$	Normalized potential applied to nozzle
$\tilde{V}$	Potential at attractor
w	Channel width

Symbols

ε_o	Permittivity of gas
ρ_e	Electric charge density

1.0 INTRODUCTION

Previous reports reviewed the earlier efforts to disperse fog [1] and examined the theoretical aspects of the charged particle fog dispersion technique in great detail [2]. The charged particle concept appeared to be a viable technique based on the review of this previous work, but it was concluded that further experimental investigation would be required to remove remaining doubts. This report details the design of a prototype charged particle fog dispersal unit and outlines the experimental program to evaluate the unit. The construction and evaluation of the unit will be performed in the next phase of this work. The techniques used to design the unit are discussed in Section 2.0, and Section 3.0 contains detailed plans for the prototype unit. The appendix contains a bibliography of work performed in electrofluid dynamic power generation that was found to be helpful in the design of the prototype unit.

2.0 DESIGN OF PROTOTYPE CHARGED PARTICLE FOG DISPERSAL UNIT

2.1 Previous Designs

Previously used charged particle fog dispersal units and their operation were described in the earlier reports [1,2] and in References [3] through [10]. This previous work will not be reviewed again here, but the results will be freely used. During the course of the design of the prototype unit the experience that had been gained by other organizations, i.e., the Curtiss-Wright Corporation, Marks Polarized Corporation, University of Dayton Research Institute, and the Aerospace Research Laboratories at Wright-Patterson Air Force Base, on the design of electrofluid dynamic (EFD) energy conversion devices was found to be of considerable assistance because of the great similarity of EFD devices and charged particle fog dispersion devices. A bibliography of work related to EFD devices is included in the appendix. Certain features of the nozzles were found to have significant influences upon increasing the amount of power generated by EFD devices. These features have been incorporated into the design of the prototype fog dispersal unit and flexibility has been included to determine whether improved performance can be obtained by utilizing these features.

2.2 Description of Prototype Unit

The features of the prototype charged particle fog dispersal unit to be described in this report are shown in Table 1. Previous investigations of fog dispersal systems [2] or electrofluid dynamic energy conversion systems (see appendix) have used various types of charge carriers (ions [3,11]; water droplets [4,5,6]; and helium bubbles [7]) that were charged either by electrostatic induction [8] or by charge transfer in a corona discharge [12,13,14,15]. The charge carriers were accelerated by electrostatic means [16] or by viscous coupling to an

TABLE 1. Features of Prototype Nozzle.

- Moist air accelerated in supersonic nozzle having fixed exit Mach number.
- Water droplets formed by homogeneous nucleation in expanding nozzle flow.
- Water droplets charged in corona discharge inside nozzle.
- Variable nozzle length to sonic radius.
- Variable corona discharge location.
- Adjustable corona needle location.
- Variable stagnation chamber specific humidity.
- Variable corona needle shape.
- Constructed from a transparent material.

accelerating airstream [17]. It was concluded from this previous work that the optimum efficiency of charge transport could be obtained by charging small water droplets in a corona discharge and accelerating these by viscous coupling with air in a supersonic nozzle [12,17].

The prototype charged particle fog dispersal unit operation will now be described in detail. Moist air is expanded through the sonic throat and expansion nozzle. At some point, condensation from spontaneous (homogeneous) nucleation occurs. Heterogeneous condensation is not usually considered an effective mechanism for nozzle flows [18]. In moist air expansions the nucleation and growth processes are uncoupled since homogeneous nucleation is over before any appreciable amount of growth has occurred [19]. The droplets grow quickly for some distance through the "condensation zone" and then more slowly up to the nozzle exit [19,20]. The location of the point where homogeneous nucleation takes place is dependent upon the average temperature gradient along the nozzle because, for a fixed exit Mach number, the amount of supercooling increases with an increase in the average temperature gradient along the nozzle ($\overline{dT/dx}$). This temperature gradient will be varied by varying the length of the nozzle.

The location for homogeneous nucleation and the droplet growth rate are extremely sensitive to the relative humidity in the stagnation region and, in addition, the droplet growth rate in the "condensation zone" depends on the length of the nozzle [18]. In general, small drops are produced in short nozzles and large drops in long nozzles. At high specific humidities it has been noted that the entire flow is foggy downstream of the condensation location. Lawson [21] found that the maximum current for electrofluid dynamic energy conversion nozzles having an exit Mach number of 2.0 was obtained with a stagnation chamber relative humidity of 17 percent. This rather low value of relative humidity required to obtain optimum results will be explained in Section 2.3.

The corona discharge must be placed after condensation has occurred and also at the location where the droplets have grown to a desirable size to be able to carry the necessary charge [2]. Therefore, several corona locations will be examined. In addition, several corona shapes will be examined and the needle location will be adjustable relative to each corona discharge location.

The nozzle will be made out of a transparent plastic in order to visualize the flow and corona discharge within the nozzle. Further explanation of the features of the prototype nozzle will be given later.

A schematic of the prototype fog dispersal nozzle is shown in Figure 1. Atmospheric air will be compressed to the proper stagnation pressure and then filtered to remove all moisture, oil droplets, and solid particles. The air then will be mixed with a controlled amount of atomized water--to control the specific humidity--in a mixing tube. The purpose of the mixing tube is to allow for complete evaporation of the water into the dry air. The swirl induced by the mixing tube will be removed by a honeycomb. The humid air will be decelerated into the stagnation chamber and then expanded through the converging/diverging nozzle until it will emerge at the nozzle exit at a supersonic Mach number. The diverging portion of the nozzle will be conical with the length much greater than the diameter at the throat. Therefore, the flow in the nozzle will be very nearly cylindrical.

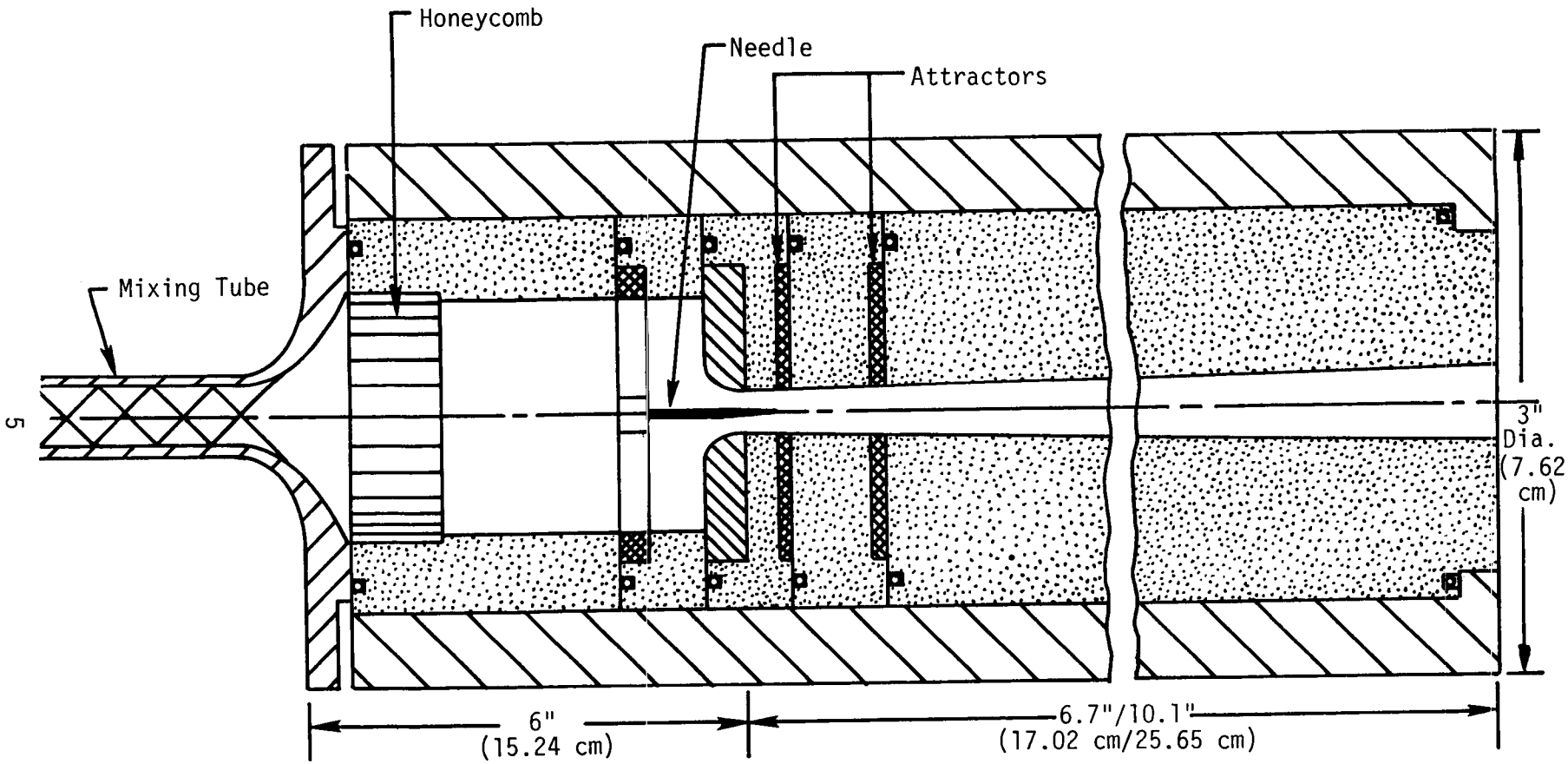

Figure 1 Prototype fog dispersal nozzle.

The water vapor will condense near the throat during the expansion process. The droplets that will be formed will be small enough to be carried by viscous drag along with the air. Thus, they will be continuously accelerated in the nozzle.

The corona needle will be attached to a veined support in the stilling chamber. The attractors can be placed at two locations and two lengths of nozzle will be examined. The overall length of the nozzle portion of the unit will be approximately 31.75 cm (12.5 in) to 40.64 cm (16 in) and 7.62 cm (3 in) in diameter. The entire system can be disassembled quickly and reassembled in a new configuration.

The estimated characteristics of the nozzle are shown in Table 2. The exit Mach number is 1.35. This is the Mach number that has been used by Gourdine [5] and the choice of the Mach number will be explained later. A 7.08×10^{-3} m^3/s (15 SCFM) compressor will be used which for an exit Mach number of 1.35 fixes the maximum diameter of the nozzle throat at 0.43 cm (0.168 in). The maximum water flow rate into air that is initially dry will be 1.42×10^{-7} m^3/s (0.135 gal/hr), which will result in a relative humidity in the stagnation region of 100 percent. The stagnation pressure will be 3.01×10^5 N/m^2 (43.6 psia) for an

TABLE 2. Nozzle Characteristics.

Exit Mach number	1.35
Minimum diameter	0.43 cm (0.168 in)
Airflow rate	7.08×10^{-3} m^3/s (15 SCFM)
Maximum water flow rate	1.42×10^{-7} m^3/s (0.135 gal/hr)
Stagnation pressure	3.01×10^5 N/m^2 (43.6 psia)
Nozzle length to sonic diameter ratio	40/60
Mach number at corona	1.07/1.15
Current (maximum)	52×10^{-6} amps
Charge to mass ratio	0.37 coul/kg

atmospheric pressure of 1.01×10^5 N/m^2 (14.7 psia). The stagnation pressure is fixed by a desire to eliminate shocks at the exit of the nozzle since shocks will result in breakup and evaporation of the water droplets. The nozzle length to diameter ratio will be 40 or 60 based on the diameter at the nozzle throat. The corona region will be placed either at a Mach number of 1.07 or 1.15. The maximum estimated current will be 52 microamps and that will result in a charge to mass ratio of 0.37 coul/kg. The exit Mach number will later be shown to be a compromise between a desire to increase the average temperature gradient along with nozzle, to increase the amount of supersaturation, and the need to keep the exit Mach number low in order to have as high a charge density as possible without a breakdown field at the exit of the nozzle.

The electrical connections to the nozzle are shown in Figure 2. The corona needle will be grounded whereas the attractor will be placed at a high but variable positive potential. This will result in a negative corona which is the desirable type of corona because of the presence of electronegative gases in air [2,22,23,24]. Microammeters will be used to measure the cathode or needle current and the attractor or anode current. The properties of the discharge will be adjusted until the attractor current is nearly zero and that will result in the maximum jet current.

The nozzle controls are shown schematically in Figure 3. The air from the compressor will be filtered to remove oil and water droplets. It will then be divided; part of the air being used to pressurize the water storage bottle and part of the air going directly into the nozzle. Water leaving the storage bottle will be strained and the flow rate will be measured with a rotameter. The water will flow through a capillary tube that will atomize the water when it meets with the air. The air/water mixture will then go through the mixing tube where the water will evaporate before reaching the nozzle. All quantities, i.e., air pressure, water pressure, and water flow rate, can be continuously controlled in order to optimize the performance of the nozzle.

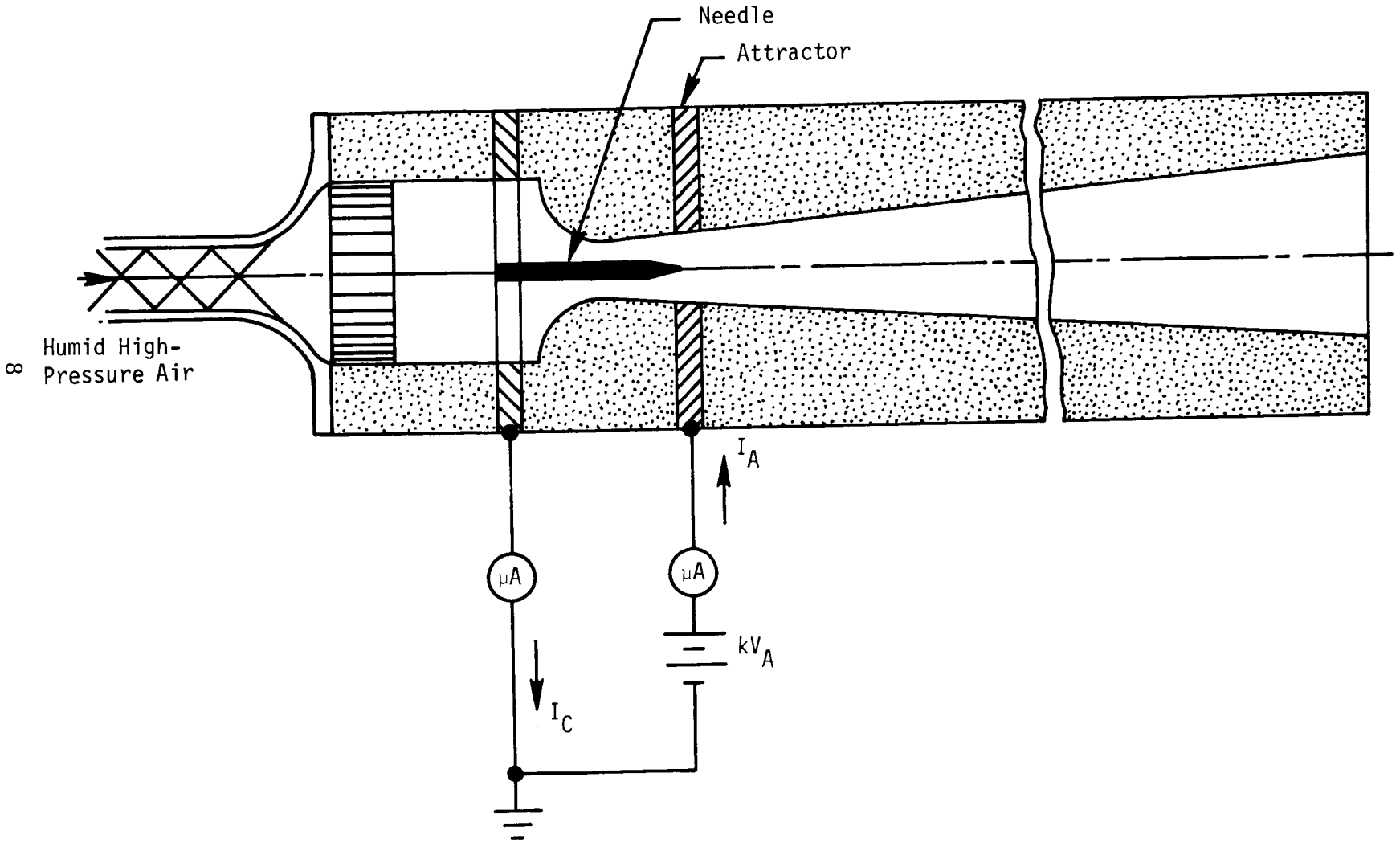

Figure 2 Schematic of charge spray nozzle.

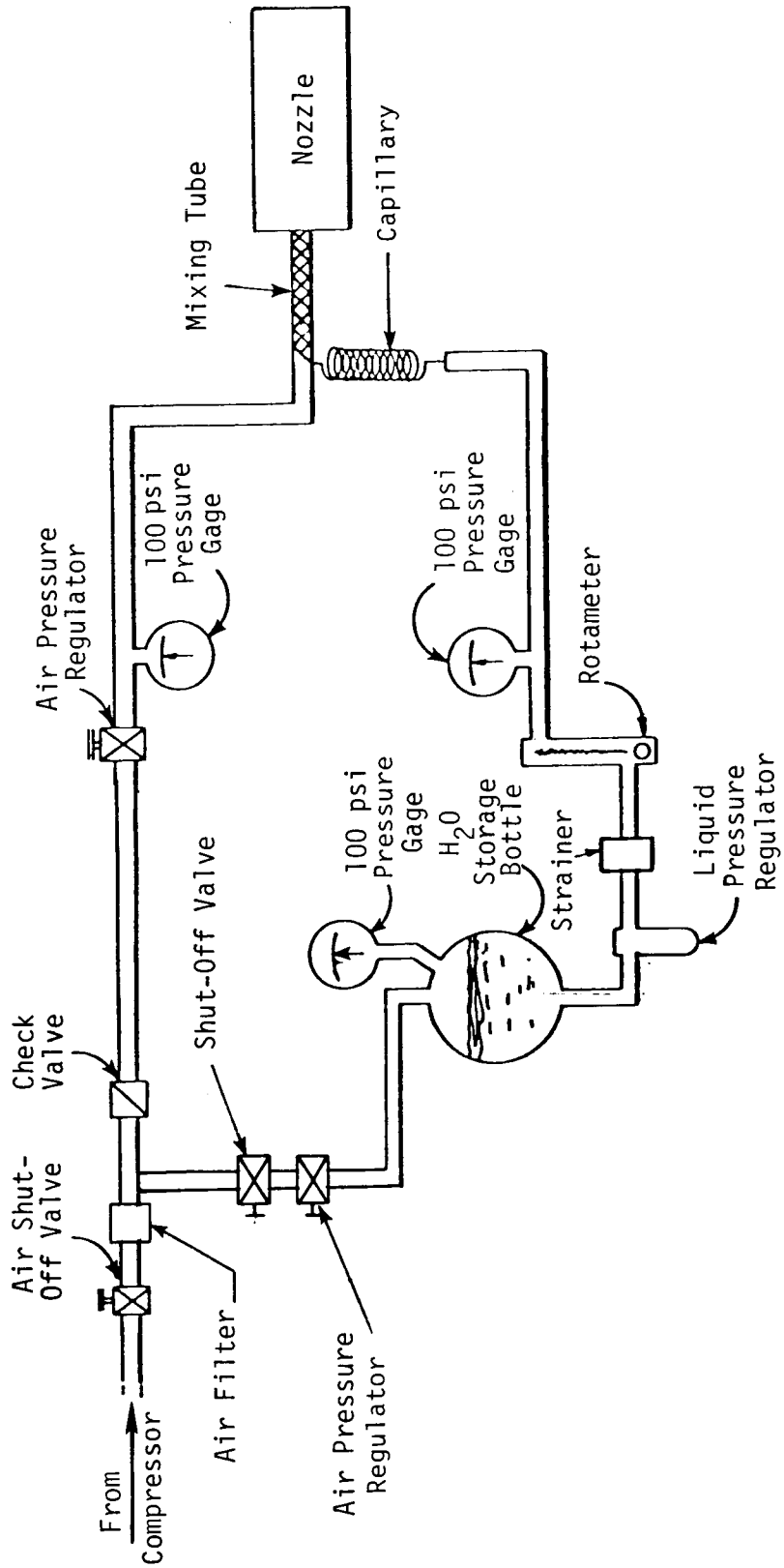

Figure 3 Nozzle controls.

2.3 Design of Prototype Unit

In this section the rationale for the design decisions that were described in the previous section will be given. First, the variable needle location is examined. Studies on electrofluid dynamic power generation devices indicated that the output current can be increased by adjusting the position of the needle relative to the attractor [25]. The apparatus used in these studies is shown in Figure 4. High-pressure air that proceeded through the corona discharge located at the nozzle sonic orifice was mixed with medium-pressure secondary air before proceeding through a grounded electrode and into the conversion duct. The configuration is shown to indicate the relative position of the corona needle to the attractor nozzle. By varying the needle location relative to the attractor nozzle, the current is found to have a maximum--as illustrated in Figure 5. Several corona needle locations relative to the attractor will be examined during testing of the nozzle.

It should also be noticed that the results shown in Figure 5 indicate that improved performance was obtained with a nail-head needle (a #8 nail was also used [21]) compared to a sharp needle. It was felt that the low-pressure region and wake that were created downstream of the nail head was advantageous for charging the droplets because the droplets were trapped for a period of time in the separated region where the corona discharge current is increased and therefore improved performance was obtained. Figure 6 indicates the geometry of the corona needles that will be examined in the study to try to obtain the maximum current from the nozzle.

It is desirable to estimate the characteristics of the droplets that can be expected to be leaving the nozzle. These estimated characteristics are shown in Table 3. The following assumptions were used in making these estimates. The water flow rate was assumed to be 1.42×10^{-7} m^3/s (0.135 gal/hr) which would give a relative humidity of 100 percent in the stagnation chamber at a temperature of 21.1° C (70° F). It was assumed that all of the droplets were charged to the breakdown field at their surface. This then allowed the number of electrical charges per particle and the mobility of the droplet to be estimated [2].

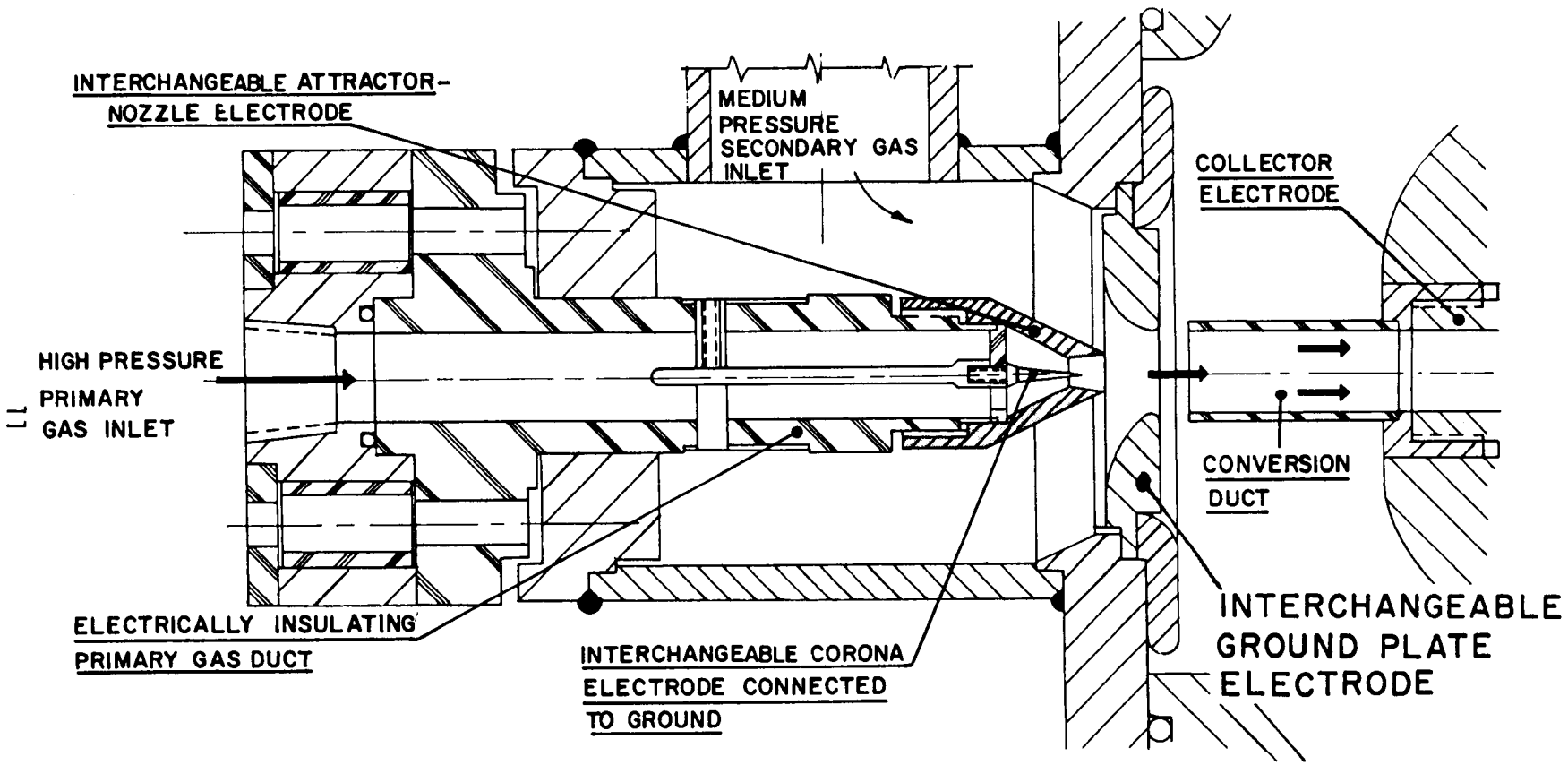

Figure 4 Typical electrode configuration of EFD test rig [25].

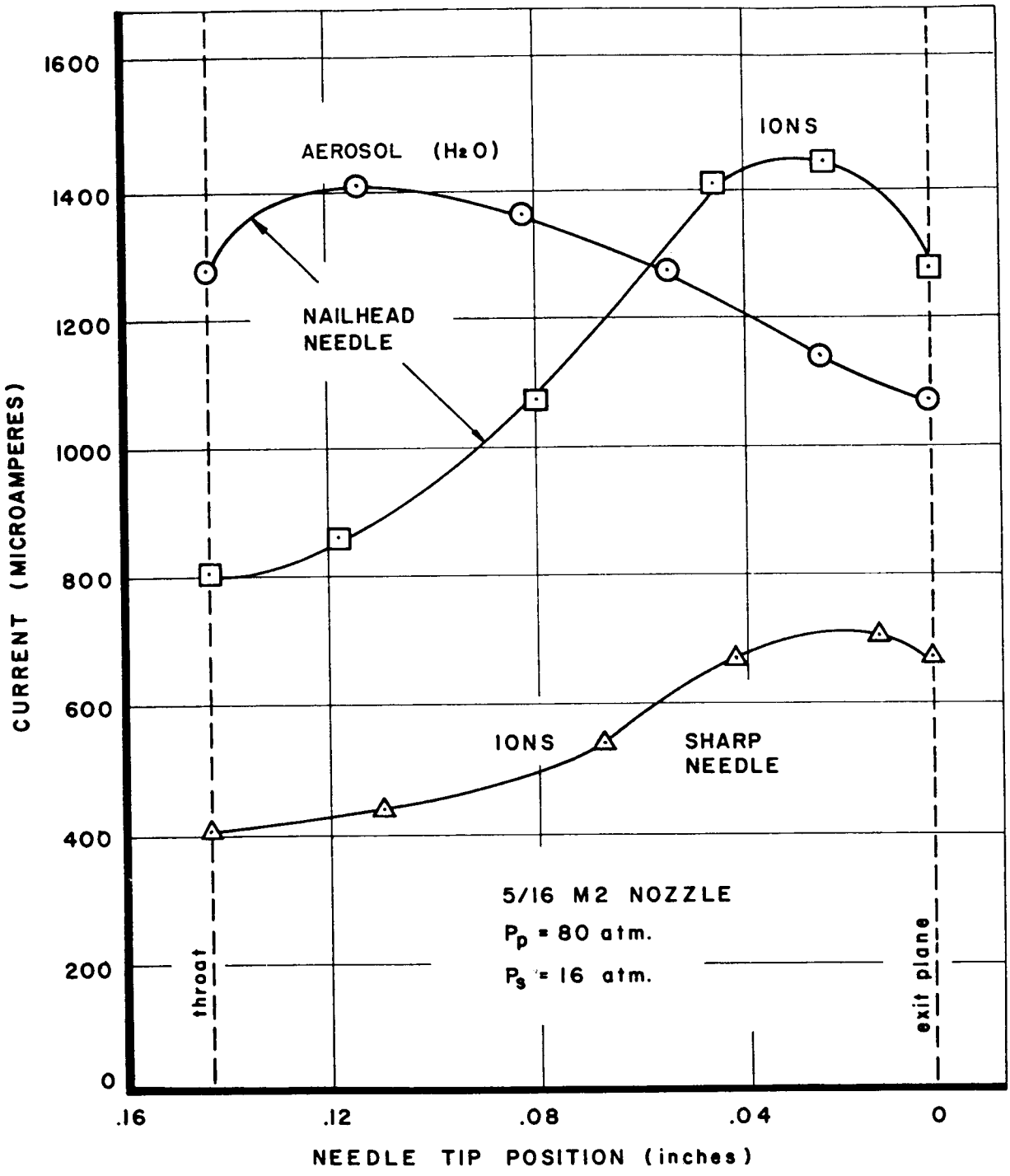

Figure 5 Current as a function of the needle position in nozzle [25].

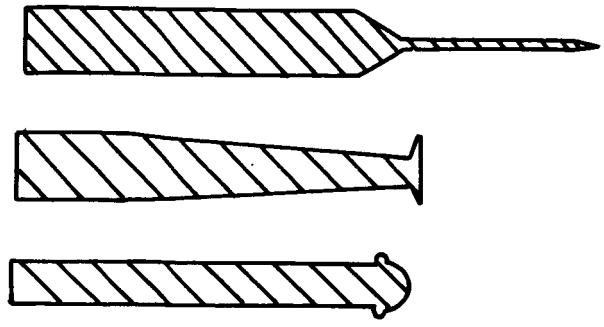

Figure 6 Corona needles.

TABLE 3. Characteristics of Nozzle Droplets.

Water flow rate = 1.42×10^{-7} m^3/s (0.135 gal/hr)
All particles charged to breakdown field at surface.

Particle Radius (m)	Particle Flux (#/sec)	Maximum Charges Per Particle (#)	Maximum Current (amp)	Mobility (m^2/volt sec)	Charge Density (coul/m^3)
5×10^{-9}	2.7×10^{17}	0.05	2.25×10^{-3}	1.10×10^{-7}	2.43×10^{-1}
10^{-8}	3.4×10^{16}	0.21	1.12×10^{-3}	1.12×10^{-7}	1.21×10^{-1}
5×10^{-8}	2.7×10^{14}	5.20	2.25×10^{-4}	1.41×10^{-7}	2.43×10^{-2}
10^{-7}	3.4×10^{13}	20.80	1.12×10^{-4}	1.82×10^{-7}	1.21×10^{-2}

Because of the Cunningham correction factor [2], the mobility is seen to be approximately constant for particles in this size range and is approximately 10^{-7} m^2/volt sec.

If the flow within the nozzle is in equilibrium, then the equilibrium drop radius can be estimated from a knowledge of the relative humidity at any particular point along the nozzle. This estimate indicates that the droplets within the nozzle are of extremely small diameter [18,19,20]. The droplets usually have diameters of 10 A° to 400 A° (1 A° = 10^{-4} microns). Therefore, the radii of the particles examined in

Table 3 are quite small, and it is felt that this is the probable range for the droplet size from these nozzles [5,19]. Thus, knowing the water flow rate, the particle flux rate can be determined, assuming spherical particles. From the maximum charge per particle and the particle flux rate, the maximum current from the nozzle can be determined.

While the calculations that were performed to obtain the results in Table 3 are straightforward, the results are in all probability incorrect because no use has been made of the equations of electrodynamics. Magnetic field effects are negligible because of the small currents and only electrostatic effects need to be considered. Therefore, the electric field is described by the Poisson equation. Minardi [26] computed the performance characteristics of electrofluid dynamic power generation nozzles assuming that the charge carrier was a colloid such as a water droplet. He assumed that he had a very long cylinder through which the gas and charged colloids flowed, that the gas velocity was constant within the long cylinder, that the charge density was constant within the cylinder, and that there was no slip velocity between the colloid and the airstream. The last assumption amounts to assuming that the mobility of the colloids is zero. Turbulent spreading and diffusion of the charged particles were neglected. The Poisson equation was then used to determine the electric field within and external to the nozzle [27,28,29]. The maximum field was found to occur at the nozzle exit.

The parameters used in his analysis are the following:

$$D = \frac{\rho_e h G}{\varepsilon_o E_{bo}} = \text{normalized charge density}$$

$$G = 1 + \frac{R}{h} - \left\{1 - \left(\frac{R}{h}\right)^2\right\}^2 = \text{configuration factor if } R/h << 1$$

$$M^* = \frac{M^2}{0.833 + 0.167M^2}$$

where ρ_e is the electric charge density, R is the radius of a channel of length h, ε_o is the permittivity of the gas, E_{bo} is the gas breakdown electric field in the stagnation chamber, M is the gas Mach number, and M* is the Mach number based on the local speed of sound.

The factor G is shown in Figure 7. For a very long channel, where the radius is much less than the length of the channel, the factor G can be approximated by the equation given and is then a very small number. Lines of constant normalized output power from the electrofluid dynamic nozzle are shown in Figure 8 as a function of M* and $\overline{V}$, the normalized potential applied to the nozzle. The results of this figure can be used in the prototype nozzle because the line $\overline{V} = 0$ gives the values of D for breakdown in the channel as a result of the charge density alone.

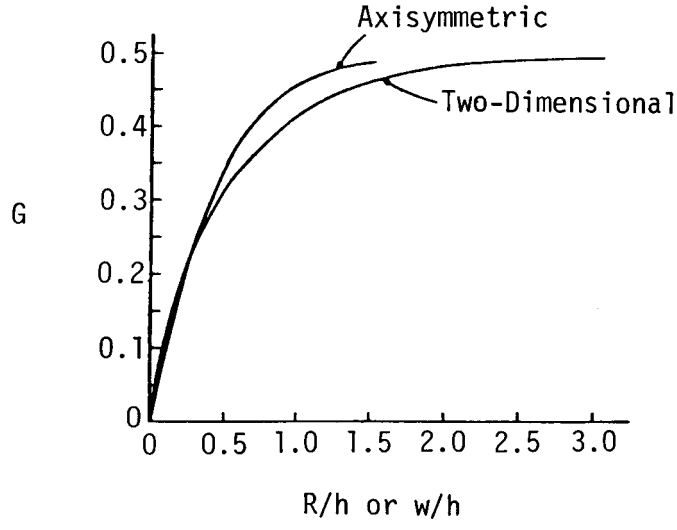

Figure 7 Configuration factor of G for both the two-dimensional and axisymmetric geometries [26].

As previously mentioned, the maximum electric field occurs at the nozzle exit and therefore breakdown will occur there first. For a given nozzle Mach number, M* can be determined. Then from Figure 8 the value of D can be obtained. It should be noted that lines of constant D intersect the M* axis at $\overline{V} = 0$. From the value of D obtained from this figure, the maximum value of the charge density within the nozzle can be determined and then the maximum current is given by

$$I_j = \rho_e V \pi R^2$$

where V is the gas velocity.

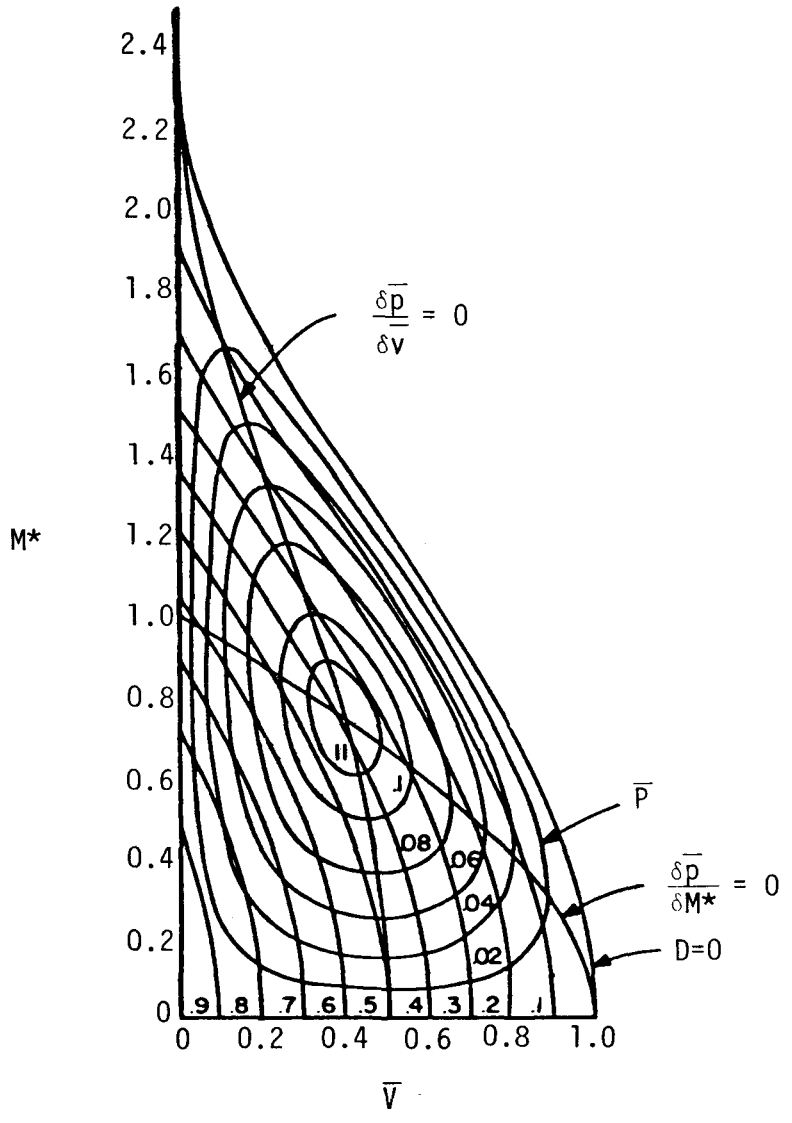

Figure 8 Lines of constant normalized power as a function of M* and $\bar{V}$ for a gas with k = 1.4. The field strength at the generator entrance is E_b [26].

The above analysis was applied to the prototype nozzle assuming that the nozzle was a cylinder with radius equal to the radius at the nozzle throat. The breakdown field was found to occur at the nozzle exit when the charge density reached 5.64×10^{-3} coul/m^3 (M* = 1.266 for an exit Mach number of 1.35) for both nozzle length to diameter ratios that will be used in the prototype nozzle. This yields a maximum prototype nozzle current of 52.3 microamps, which is considerably less than

the estimated currents shown in Table 3. This maximum nozzle current would occur for any particle radius within the range considered and it therefore appears that the nozzle current is controlled by the breakdown of the field at the nozzle exit rather than the details of the charging process, provided it is sufficiently efficient. In addition, under the assumptions that were made in calculating Table 3, it is seen that the stagnation chamber relative humidity can be greatly reduced and the nozzle will deliver the same current (2.3 percent for 5×10^{-9} m radius droplets to 47 percent for 10^{-7} m radius droplets), i.e., the water flow rate can be greatly reduced. Lawson obtained optimum results with a relative humidity of 17 percent [21].

As a verification of the applicability of this analysis to the current from a fog dispersal nozzle, it was applied to the nozzle used by Gourdine [5]. The analysis estimates that the maximum current would be 99 microamps while the current was measured to be 100 to 135 microamps. Therefore, it is felt that the analysis of Minardi can be applied to the prototype nozzle and will give a reasonably accurate estimate of the maximum current that can be expected from the nozzle. During testing, the various features of the prototype nozzle will be studied to determine the maximum current the nozzle will deliver.

Notice that Figure 8 indicates that the value of D for breakdown of the field at the exit decreases as M* increases or as the Mach number of the nozzle exit increases. Therefore, increased charge density can be obtained by lowering the Mach number. But the condensation process requires a minimum value of the mean temperature gradient across the nozzle, which decreases as the exit Mach number is increased (for a fixed length to sonic diameter ratio). Gourdine [5] used nozzles having an exit Mach number of 1.35 and it is proposed that the prototype nozzle that is described in this report have the same Mach number since this appears to be a good compromise between these two competing effects.

It was desired to choose a size for the prototype nozzle that could be economically manufactured in large numbers and would also place the required number of charges into the fog in a reasonable length of time. The design trade-offs that are possible can be obtained by examining the

scaling laws for the corona discharge [12,22]. These scaling laws, which are summarized in Table 4, indicate the effect of varying the nozzle dimensions and the stagnation pressure upon the discharge. If the dimensions of the nozzles are doubled, then the current can be increased by a factor of two. However, the nozzle area then has been increased by a factor of four which results in a four-fold increase in the air volume flow rate in standard cubic feet per minute. This then requires a compressor of four times capacity. However, that compressor is approximately four times as expensive as the one for the original nozzle while leading to only a doubling of the nozzle current. Therefore, nozzles of a moderate size are more economical than half the number of nozzles that are twice as large since the compressor is the most expensive component. Gourdine suggested that the medium-sized nozzles that he had examined would be suitable for an airport application [30,31]. Because of the availability of a reliable 7.08 x 10^{-3} m^3/s (15 SCFM) compressor, the prototype nozzle was designed for that capacity

TABLE 4. Corona Scaling Laws.

Increase all dimensions by a factor α:
$\rho_{e,\alpha} = \frac{\rho_e}{\alpha}$
$I_{j,\alpha} = \alpha I_j$
Increase pressure from p_N to p:
$E_b = E_{b,N} \frac{p}{p_N}$ breakdown field (Paschen's law)
$\rho_e = \rho_{e,N} \frac{p}{p_N}$
$\tilde{V} = \tilde{V}_N \frac{p}{p_N}$ potential on attractor
$I = I_N \frac{p}{p_N}$

with an exit Mach number of 1.35. The other expected characteristics of the prototype nozzle are given in Table 2.

The unit has been designed to allow for the variation of the features listed in Table 1. In addition, attention has been paid to making the unit easily modified to allow optimization of the design.

3.0 DRAWINGS OF PROTOTYPE CHARGED PARTICLE FOG DISPERSAL UNIT

Detailed drawings of the prototype unit are shown in Figures 9, 10, and 11. The nozzle unit will be constructed of machined and polished plexiglas units that will be sealed with O-rings. The unit will be bolted together using threaded rods. Connections to the prototype nozzle will be constructed from commercially available pipe fittings. The entire control unit and the nozzle will be mounted on handtrucks to make the unit portable.

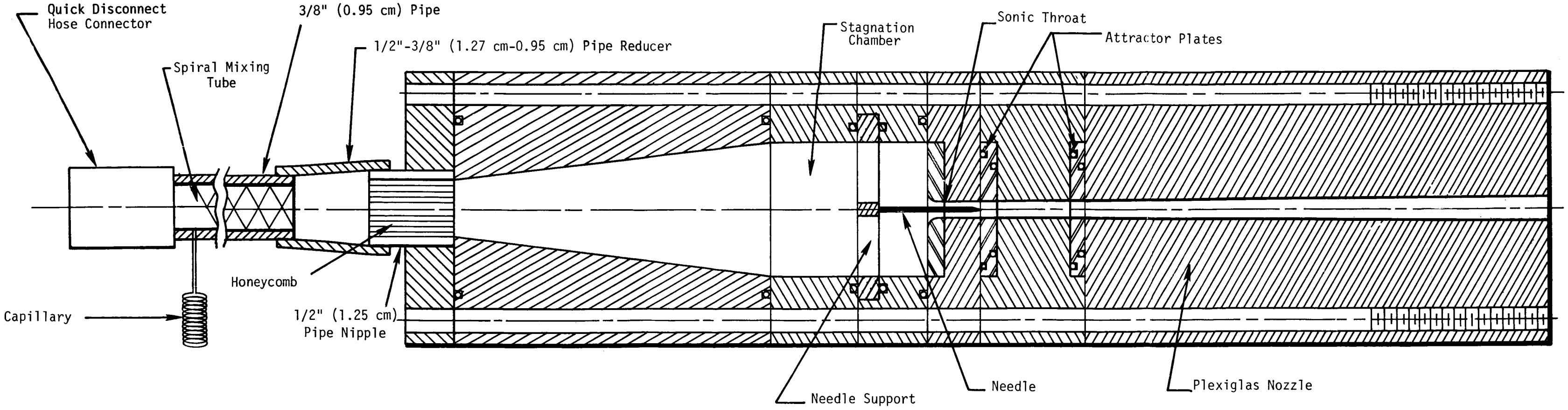

Figure 9 Cross section of prototype nozzle.

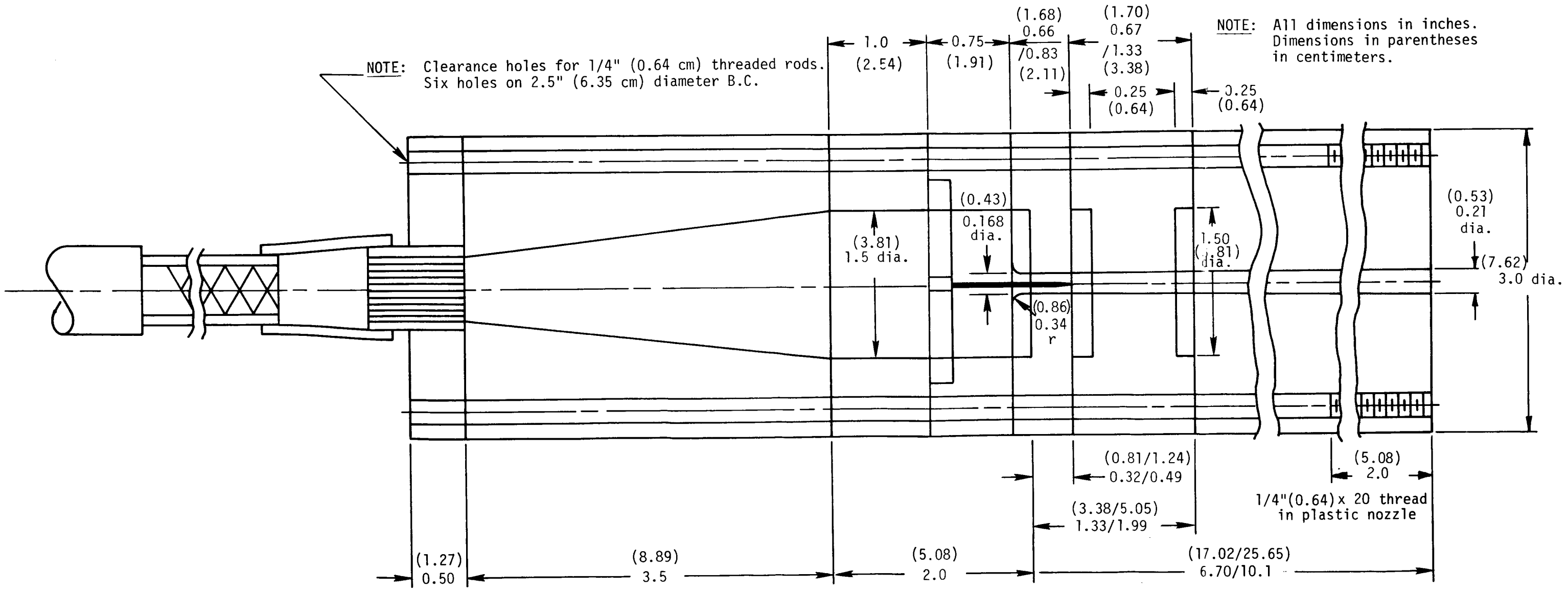

Figure 10 Details of prototype nozzle.

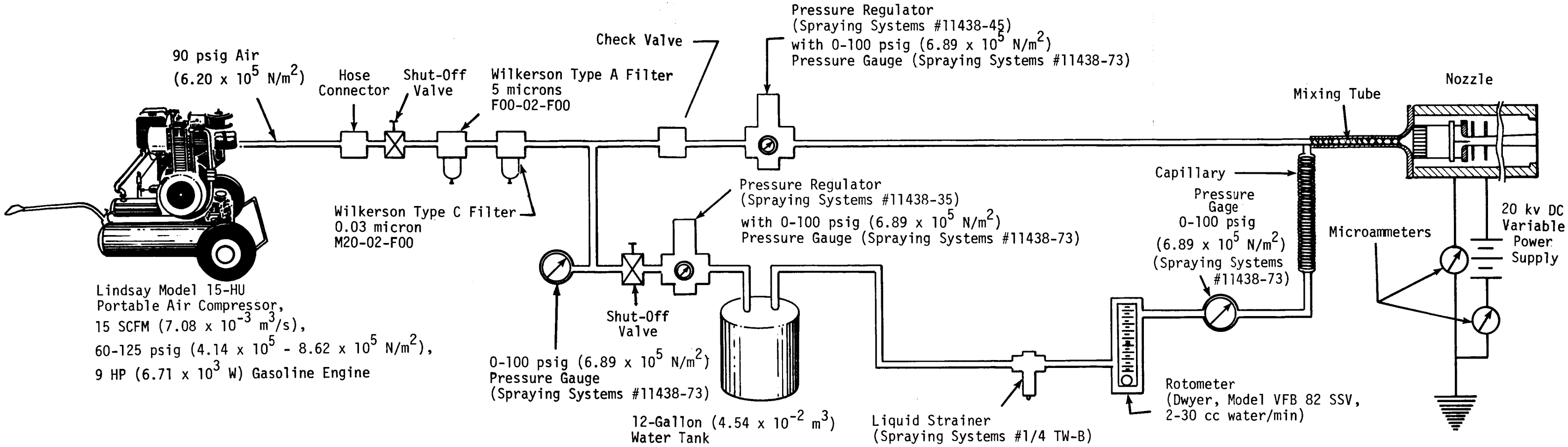

NOTE: All plumbing is 1/4" (0.64 cm) galvanized steel pipe.

Figure 11 Details of prototype fog dispersal system.

4.0 DESIGN OF VERIFICATION EXPERIMENTS FOR FOG DISPERSAL UNIT

The performance of the nozzle must be completely measured. The purpose of the measurements will be to learn how to maximize the current from the nozzle under various conditions of corona location and potential and stagnation chamber relative humidity to determine the electric field that is created external to the nozzle and to determine the effect of the electric field on fog. The nozzle performance can be determined from laboratory measurements, but the external field measurements need to be performed both at specialized facilities (fog chambers) and in the atmosphere. It is preferable to perform controlled measurements in a fog chamber before performing atmospheric measurements. The quantities to be measured are listed in Table 5.

The nozzle will be operated at a constant pressure ratio (stagnation to atmospheric pressure). This ratio is fixed by the exit Mach number so that the exit pressure is equal to the atmospheric pressure, thus eliminating compression or rarefaction waves at the exit. The nozzle flow rate is fixed by the pressure ratio and the minimum nozzle area since the nozzle is choked. The stagnation pressure is controllable and can be set corresponding to any measured atmospheric pressure. The stagnation chamber relative humidity is controlled by first drying the air entering the stagnation chamber and then adding controlled amounts of water. The water flow rate is measured with the rotameter on the control panel. The stagnation chamber temperature must also be measured to determine the relative humidity and it will be measured with a thermocouple in the stagnation chamber. No practical methods exist for measuring the size of the submicron particles that are leaving the nozzle exit [19]. The particle size will be inferred from measured charge to mass ratios and by using diffusion charging or electric field breakdown theory. Also the possibility of droplet size measurement with laser techniques will be investigated. The attractor, needle, and nozzle exit currents will be measured with commercial microammeters. In addition,

TABLE 5. Quantities to be Measured.

Nozzle Properties:

- Stagnation pressure
- Stagnation temperature
- Stagnation relative humidity
- Exit Mach number
- Exit droplet size

Electrical Properties:

- I_C, I_A, I_j
- Charge density distribution
- Electric field distribution

Atmospheric Properties:

- Pressure
- Temperature
- Relative humidity
- Visibility
- Wind velocity

the electric field and the charge density external to the nozzle must be measured before the nozzle is turned on and during the operation of the nozzle. Ideally, the distribution of both quantities must be measured to verify the various theories about the external field [2]. This is difficult to do because of the interference between the measuring instrument and its support and connection to the ground and the field to be measured, but these effects can be minimized by calibration of the instruments in place.

The vertical component of the static electric field will be measured using field mills [32,33,34,35]. The number of field mills to be used will depend somewhat on their availability. The field mills will be required to either have a large dynamic range (10 to 10^6 volt/m) or two different sets of instruments will have to be used so that both the background field and the field due to the charged droplets can be measured. The field mills will have to be calibrated both in the laboratory and in place in the field. They will be calibrated by fitting large plates to them and applying a DC voltage between the plates. Comparison

with a laboratory-calibrated field mill will be required in the field because of the influence of the field mounting upon the calibration.

It is also necessary to measure the space-charge distribution in the atmosphere in the region of the nozzle. A cage technique was used by Gourdine [5] and appears to be the most useful method to measure the charge density at considerable heights above the ground [36]. Calibration is difficult but comparison can be made between the estimates of the charge density using the measurements of the electrical field and Poisson's equation and the cage measurement.

The remaining atmospheric measurements indicated in Table 5 will be made using standard techniques. The complete field program was described previously [2].

5.0 CONCLUDING REMARKS

The detailed design of a prototype charged particle fog dispersal unit has been presented in this report. The concepts used for the design are well understood and have been widely used in the past both for fog dispersal units and for electrofluid dynamic power generation. Therefore, it is anticipated that the prototype unit will work efficiently as a current source over a wide range of conditions. However, the characteristics of the prototype unit that will ensure efficient dispersal of an atmospheric fog of given properties are still not known. In particular, the optimum water droplet size is unknown. Part of the uncertainty results from a lack of knowledge of how a fog is dispersed by the charged droplets. It is possible that it is dispersed by coalescence and subsequent movement in the gravitational field to the ground [9,10] or the droplets could transfer part of their charge to the fog particles causing them to follow the electric field to the ground [30]. Also, it is possible that only some coalescence is required to increase the visibility through the fog without precipitation. Different mechanisms quite possibly could be involved in fog dispersal in different types of fogs. These questions must be addressed in a full field test of a group of prototype units. Only a sufficiently large group of units which create a nearly uniform electric field distribution in the horizontal direction will fully verify the two-dimensional fog dispersal theories [30]. The number of units to be used is dependent on the performance results from the prototype unit. Thus, the more complete field tests should be performed only after complete examination of the single unit that is described in Section 4.0.

REFERENCES

1. Christensen, Larry S., and Walter Frost: "Fog Dispersion," NASA CR-3255, March, 1980.

2. Frost, Walter, Frank G. Collins, and David Koepf: "Charged Particle Concepts for Fog Dispersion," NASA CR 3440, June, 1981.

3. Ruhnke, L. H.: "Warm Fog Modification by Seeding with Unipolar Ions," AMS Second National Conference on Weather Modification, Santa Barbara, California, pp. 385-388, 1970.

4. Juisto, J. E.: "Laboratory Evaluation of an Electrogasdynamic Fog Dispersal Concept," Federal Aviation Administration Report No. FAA-RD-72-99, 1972.

5. Chiang, T. K.: "Field Evaluation of an Electrogasdynamic Fog Dispersal Concept, Part I," Federal Aviation Administration Report No. FAA-RD-73-33, February, 1973.

6. Wright, T., and R. Clark: "Field Evaluation of an Electrogasdynamic Fog Dispersal Concept, Part II," Federal Aviation Administration Report No. FAA-RD-73-33, February, 1973.

7. Clark, R. S., et al.: "Project Foggy Cloud V: Panama Canal Warm Fog Dispersal Program," Naval Weapons Center Report NWC TP 5542, December, 1973.

8. Carroz, John W., and Patrick N. Keller: "Electrostatic Induction Parameters to Attain Maximum Spray Charge to Clear Fog," Naval Weapons Center Report NWC TP 5796, January, 1976.

9. Tag, Paul M.: "A Numerical Simulation of Warm Fog Dissipation by Electrically Enhanced Coalescence: Part I. An Applied Electric Field," Journal of Applied Meteorology, Vol. 15, pp. 282-291, 1976.

10. Tag, Paul M.: "A Numerical Simulation of Warm Fog Dissipation by Electrically Enhanced Coalescence: Part II. Charged Drop Seeding," Journal of Applied Meteorology, Vol. 16, pp. 683-696, 1977.

11. Whitby, K. T.: "Generator for Producing High Concentrations of Small Ions," The Review of Scientific Instruments, Vol. 32, pp. 1351-1355, 1961.

12. Lawson, Maurice O.: "Ion Generation by Corona Discharge for Electro-Fluid Dynamic Energy Conversion Processes," Aerospace Research Laboratories Report ARL 64-76, October, 1964; Proceedings of the Sixth AGARD Combustion and Propulsion Colloquium, March 16-20, 1964, Cannes, France, pp. 603-612.

13. Kahn, Bernard, and Meredith C. Gourdine: "Electrostatic Power Generation," AIAA Journal, Vol. 2, pp. 1423-1427, 1964.

14. Marks, A., E. Barreto, and C. K. Chu: "Charged Aerosol Energy Convecter," AIAA Journal, Vol. 2, pp. 45-51, 1964.

15. Marks, Alvin M.: "Optimum Charged Aerosols for Power Conversion," Journal of Applied Physics, Vol. 43, pp. 219-230, 1972.

16. Hasingei, Seigfried: "Performance Characteristics of Electro-Ballistic Generators," Proceedings of the Sixth AGARD Combustion and Propulsion Colloquium, March 16-20, 1964, Cannes, France, pp. 581-601.

17. Lawson, Maurice O.: "Performance Characteristics of Electro-Fluid Dynamic Energy Conversion Processes Employing Viscous Coupling," Proceedings of the Sixth AGARD Combustion and Propulsion Colloquium, March 16-20, 1964, Cannes, France, pp. 563-580.

18. Wegener, P. P., and L. M. Mack: "Condensation in Supersonic and Hypersonic Wind Tunnels," Advances in Applied Mechanics, Vol. 5, H. L. Dryden and T. von Karman (editors). New York: Academic Press, 1958.

19. Moses, C. A., and G. D. Stein: "On the Growth of Steam Droplets Formed in a Laval Nozzle Using Both Static Pressure and Light Scattering Measurements," Transactions of the ASME, Journal of Fluids Engineering, Vol. 100, pp. 311-322, 1978.

20. Barreto, Ernesto: "On the Formation of Langevin Ions in Water Supersaturated Air Jets," Final report, ONR Contract Nonr-4890(00), AD670551, 1968.

21. Lawson, Maurice O.: Private communication, December 18, 1980.

22. Howartson, A. M.: An Introduction to Gas Discharges. New York: Pergamon Press, 1965.

23. Loeb, Leonard B.: Electrical Coronas, Their Basic Physical Mechanisms. Berkeley, California: University of California Press, 1965.

24. Goldman, M., and A. Goldman: "Corona Discharges," Chapter 4, Gaseous Electronics, Vol. 1, Merle N. Hirsh and H. J. Oskam (editors). New York: Academic Press, 1978.

25. Decaire, John A.: "Effects of Electrode Geometry-Similarity and Scaling Laws in EFD Energy Conversion Processes, I. Fundamental Considerations," AGARDograph 122, Selected Topics in Electro-fluid Dynamic Energy Conversion, December, 1968.

26. Minardi, J. E.: "Computed Performance Characteristics of Electro-fluid Dynamic Colloid Generators," Transactions of the ASME, Journal of Engineering for Power, pp. 183-191, April, 1971.

27. Hamza, Vladimir, and Edward A. Richley: "Numerical Solution of Two-Dimensional Poisson Equation: Theory and Application to Electrostatic-Ion-Engine Analysis," NASA TN D-1323, October, 1962.

28. Hamza, Vladimir: "Numerical Solution of Axially Symmetric Poisson Equation: Theory and Application to Ion-Thrustor Analysis," NASA TN D-1711, May, 1963.

29. Bogart, Carl, D., and Edward A. Richley: "A Space-Charge-Flow Computer Program," NASA TN D-3394, April, 1966.

30. Gourdine, M. C., T. K. Chiang, and A. Brown: "A Critical Analysis of the EGD Fog Dispersal Technique," The Cornell Engineer, pp. 14-34, November, 1975.

31. Gourdine, Meredith C.: Private communication, June 25, 1980.

32. Malan, D. J., and B. F. J. Schonland: "An Electrostatic Fluxmeter of Short Response-Time for Use in Studies of Transient Field-Charges," Phys. Soc. Proceedings, Section B, Vol. 63, pp. 402-408, 1950.

33. Mapleson, W. W., and W. S. Whitlock: "Apparatus for the Accurate and Continuous Measurement of the Earth's Electric Field," Journal of Atmospheric and Terrestrial Physics, Vol. 7, pp. 61-72, 1955.

34. Gathman, Stuart G., and Robert V. Anderson: "Improved Field Meter for Electrostatic Measurements," The Review of Scientific Instruments, Vol. 36, pp. 1490-1493, 1965.

35. Anderson, R. B.: "Measuring Techniques," Lightning, Vol. 1, Chapter 13, R. H. Golde (editor). New York: Academic Press, 1977.

36. Chalmers, J. Alan: Atmospheric Electricity, 2nd edition. New York: Pergamon Press, 1967.

APPENDIX

APPENDIX

BIBLIOGRAPHY OF WORK RELATED TO ELECTROFLUID DYNAMIC POWER GENERATION

1. Bogart, Carl D., and Edward A. Richley: "A Space-Charge-Flow Computer Program," NASA TN D-3394, April, 1966.

2. Decaire, John A.: "Effects of Electrode Geometry-Similarity and Scaling Laws in EFD Energy Conversion Processes, I. Fundamental Considerations," AGARDograph 122, Selected Topics in Electrofluid Dynamic Energy Conversion, December, 1968.

3. Hamza, Vladimir, and Edward A. Richley: "Numerical Solution of Two-Dimensional Poisson Equation: Theory and Application to Electrostatic-Ion-Engine Analysis," NASA TN D-1323, October, 1962.

4. Hamza, Vladimir: "Numerical Solution of Axially Symmetric Poisson Equation: Theory and Application to Ion-Thrustor Analysis," NASA TN D-1711, May, 1963.

5. Hasingei, Siegfried: "Performance Characteristics of Electro-Ballistic Generators," Proceedings of the Sixth AGARD Combustion and Propulsion Colloquium, March 16-20, 1964, Cannes, France, pp. 581-601.

6. Hawes, M.: "Experimental Techniques in Electrofluid Dynamic Energy Conversion Research," Proceedings of the Sixth AGARD Combustion and Propulsion Colloquium, March 16-20, 1964, Cannes, France, pp. 613-630; Aerospace Research Laboratories Report ARL 64-77, October, 1964.

7. Kahn, Bernard, and Meredith C. Gourdine: "Electrogasdynamic Power Generation," AIAA Journal, Vol. 2, pp. 1423-1427, 1964.

8. Lawson, Maurice O.: "Performance Characteristics of Electro-Fluid Dynamic Energy Conversion Processes Employing Viscous Coupling," Proceedings of the Sixth AGARD Combustion and Propulsion Colloquium, March 16-20, 1964, Cannes, France, pp. 563-580.

9. Lawson, Maurice O.: "Ion Generation by Corona Discharge for Electro-Fluid Dynamic Energy Conversion Processes," Aerospace Research Laboratories Report ARL 64-76, October, 1964; Proceedings of the Sixth AGARD Combustion and Propulsion Colloquium, March 16-20, 1964, Cannes, France, pp. 603-612.

10. Marks, A., E. Barreto, and C. K. Chu: "Charged Aerosol Energy Convecter," AIAA Journal, Vol. 2, pp. 45-51, 1964.

11. Marks, Alvin M.: "Optimum Charged Aerosols for Power Conversion," Journal of Applied Physics, Vol. 43, pp. 219-230, 1972.

12. Minardi, J. E.: "Computed Performance Characteristics of Electrofluid Dynamic Colloid Generators," Transactions of the ASME, Journal of Engineering for Power, pp. 183-191, April, 1971.

13. Minardi, J. E., and M. O. Lawson: "Research Progress on the Electrofluid Dynamic Wind Generator," Paper presented at SERI Second Wind Energy Innovative Systems Conference, December 3-5, 1980, Colorado Springs, Colorado.

14. Stuetzer, Otmar M.: "Ion Drag Pressure Generation," Journal of Applied Physics, Vol. 30, pp. 984-994, 1959.

15. Stuetzer, Otmar M.: "Ion Transport High Voltage Generators," The Review of Scientific Instruments, Vol. 32, pp. 16-22, 1961.

16. Willke, Theodore L.: "Current Production in a Cylindrical Geometry Electrofluid Dynamic Generator," Aerospace Research Laboratories Report ARL 71-0245, October, 1971.

17. Wifall, James R.: "Effects of Electrode Geometry-Similarity and Scaling Laws in EFD Energy Conversion Processes, II. Experimental Results," AGARDograph 122, Selected Topics in Electrofluid Dynamic Energy Conversion, December, 1968.

TECHNICAL REPORT STANDARD TITLE PAGE

1. REPORT NO.	2. GOVERNMENT ACCESSION NO.	3. RECIPIENT'S CATALOG NO.
NASA CR-3481		

4. TITLE AND SUBTITLE	5. REPORT DATE
DESIGN OF PROTOTYPE CHARGED PARTICLE FOG DISPERSAL UNIT	December 1981
	6. PERFORMING ORGANIZATION CODE
7. AUTHOR(S)	8. PERFORMING ORGANIZATION REPORT #
Frank G. Collins, Walter Frost, and Philip Kessel	
9. PERFORMING ORGANIZATION NAME AND ADDRESS	10. WORK UNIT NO.
FWG Associates, Inc. R.R. 2, Box 271-A Tullahoma, Tennessee 37388	M-364
	11. CONTRACT OR GRANT NO. NAS8-33541
	13. TYPE OF REPORT & PERIOD COVERED
12. SPONSORING AGENCY NAME AND ADDRESS	Contractor Report
National Aeronautics and Space Administration Washington, D.C. 20546	14. SPONSORING AGENCY CODE

15. SUPPLEMENTARY NOTES

Marshall Technical Monitor: Dennis W. Camp
Final Report

16. ABSTRACT

A prototype charged particle fog dispersal unit was designed, and drawings of the unit are included. Experience gained by previous investigators on charged particle fog dispersal techniques and on electrofluid dynamic energy conversion devices was incorporated into the design. The unit was designed to be easily modified so that certain features that influence the output current and particle size distribution could be examined. An experimental program was designed to measure the performance of the unit. The program includes measurements in a fog chamber and in the field. Unit performance parameters plus external electric field quantities must be measured.

17. KEY WORDS	18. DISTRIBUTION STATEMENT
Fog Fog Dispersal Visibility Ceilings Cloud Physics	Unclassified - Unlimited Subject Category 47

19. SECURITY CLASSIF. (of this report)	20. SECURITY CLASSIF. (of this page)	21. NO. OF PAGES	22. PRICE
Unclassified	Unclassified	40	A03